Processing and Application of Ceramics 9 [1] (2015) 43–51
DOI: 10.2298/PAC1501043O

Synthesis of iron doped titanium dioxide by sol-gel method for magnetic applications

Karen Oganisian[1,*], Agnieszka Hreniak[2], Andrzej Sikora[2], Dominika Gaworska-Koniarek[2], Agnieszka Iwan[2,*]

[1]*Institute of Low Temperature and Structure Research, PAS, Okolna 2, 50-422 Wroclaw, Poland*
[2]*Electrotechnical Institute, Division of Electrotechnology and Materials Science, M. Sklodowskiej-Curie 55/61 Street, 50-369 Wroclaw, Poland*

Received 19 January 2015; Received in revised form 2 March 2015; Received in revised form 24 March 2015; Accepted 27 March 2015

Abstract

In this paper magnetic properties of six TiO_2 powders doped with 1, 5 and 10 mol% Fe and prepared by sol-gel method in two different ways were analysed. The size of the obtained TiO_2:Fe particles was in the range 200–350 nm as it was confirmed by SEM and AFM techniques. The magnetization of nanopowders was measured as a function of temperature (1.8–300 K) and applied magnetic field. The samples with low Fe content manifest superparamagnetic dependence of magnetization. Whereas, the other compounds exhibit the paramagnetic behaviour with the negative Curie temperature, that suggests the antiferromagnetic ordering. Mass susceptibility decreased with the increase of Fe content as an effect of reduction of the mobility and number of charge carriers. The measurements showed that magnetic properties are correlated much stronger with the synthesis method than with the grain size.

Keywords: *TiO_2, Fe-doping, nanoparticles, AFM, magnetic properties*

I. Introduction

Titanium dioxide has been widely studied and used in different applications such as a photocatalytic material for self-cleaning coatings, environmental purifiers, antifogging mirrors and many others [1,2]. Taking into the consideration the practical application of TiO_2, a lot of work have been dedicated to obtain titanium dioxide doped with different ions, such as Ag, Cu or Ni [1–9]. Iron has also been used for synthesis of doped-TiO_2 [10–19]. Also, several methods have been developed to prepare Fe_2O_3-TiO_2 particles. For example, Liu *et al.* [18] prepared the Fe-doped TiO_2 nanorod clusters and monodispersed nanoparticles by a modified hydrothermal and solvothermal method. Shi *et al.* [19] obtained Fe-La-TiO_2 photocatalysts by a sol-gel method. Some researchers have proposed doping TiO_2 with transition metals as a way to shift the absorption edge to longer wavelengths [10–19]. Moreover, an effort has been dedicated to doping TiO_2 with Fe(III) [11–13]. For example, Ranjit and Viswanathan [11] have indicated that Fe(III)-doped TiO_2 improves photocatalytic activity up to a certain doping level (1.8 wt.%) of Fe(III).

The main goal of this work was the investigation of the influence of the amount of Fe and synthesis method on the magnetic properties of TiO_2 powder as a function of temperature (1.8–300 K) and applied magnetic field. A special emphasize was put to investigate the obtained TiO_2:Fe powders via AFM technique including magnetic force microscopy (MFM) method.

II. Experimental

2.1. Synthesis

Titania powders doped with 1, 5 and 10 mol% Fe (TiO_2:Fe x% where x = 1, 5 and 10) were obtained by using two methods of synthesis. In both cases components such as titanium(IV)-isopropoxide (TIPO) (99+% purchased from Alfa Aesar), ethanol, and distilled water were applied and stirred during 4 hours. Difference in both methods of synthesis was only the starting point

* Corresponding authors: tel: +48 713283061
e-mail: *a.iwan@iel.wroc.pl* (A. Iwan)
e-mail: *k.oganisian@int.pan.wroc.pl* (K. Oganisian)

of $Fe(NO_3)_3 \times 9\,H_2O$ addition to the mixture. In the first method $Fe(NO_3)_3$ (purchased from POCh Gliwice) was added at the beginning of synthesis, while in the second case $Fe(NO_3)_3$ was added to sol mixture 2 hours after the beginning of synthesis and stirred for another 2 hours. Details of the TiO_2:Fe synthesis are presented below.

The iron doped titania powders synthesized by the first method (TiO_2:Fe x%-a, where x = 1, 5 and 10) were prepared by sol-gel method. Briefly, 4.5 ml of titanium(IV)-isopropoxide (TIPO) dissolved in 21 ml of ethanol was mixed with 3.5 ml of distilled water and $Fe(NO_3)_3$ to obtain sol with the molar ratio $Fe(NO_3)_3$/TIPO equal to 1%, 5% and 10%. The solution was stirred in a plastic flask at room temperature for 4 h. During the stirring, the titanium dioxide powder was formed and after filtering dried at room temperature. The obtained TiO_2:Fe x%-a powders were heated at 500 °C for one hour.

The iron doped titania powders synthesized by the second method were abbreviated as TiO_2:Fe x%-b (where x = 1, 5 and 10). Briefly, 4.5 ml of TIPO and 21 ml of ethanol were mixed with 3.5 ml of distilled water yielding a titania sol. The solution was stirred in a plastic flask at room temperature for 2 h. Then, $Fe(NO_3)_3$ was added to the obtained sol (the molar ratio $Fe(NO_3)_3$/TIPO equal to 1%, 5%, 10%) and mixed for another 2 h. During the stirring, titania particles were formed and after filtering dried at room temperature. The TiO_2:Fe x%-b powders were finally heated at 500 °C for one hour.

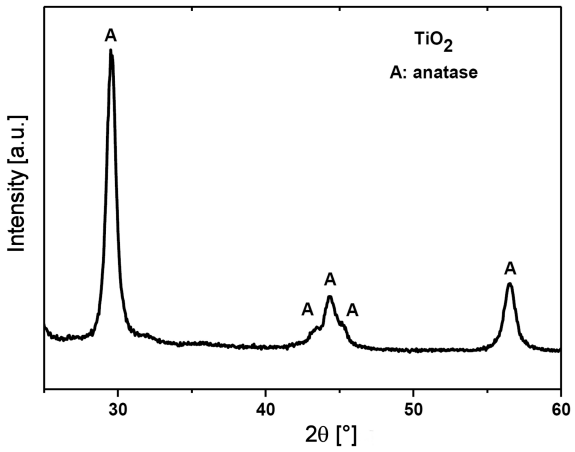

Figure 1. X-ray pattern of pure TiO_2 powder annealed at 500 °C

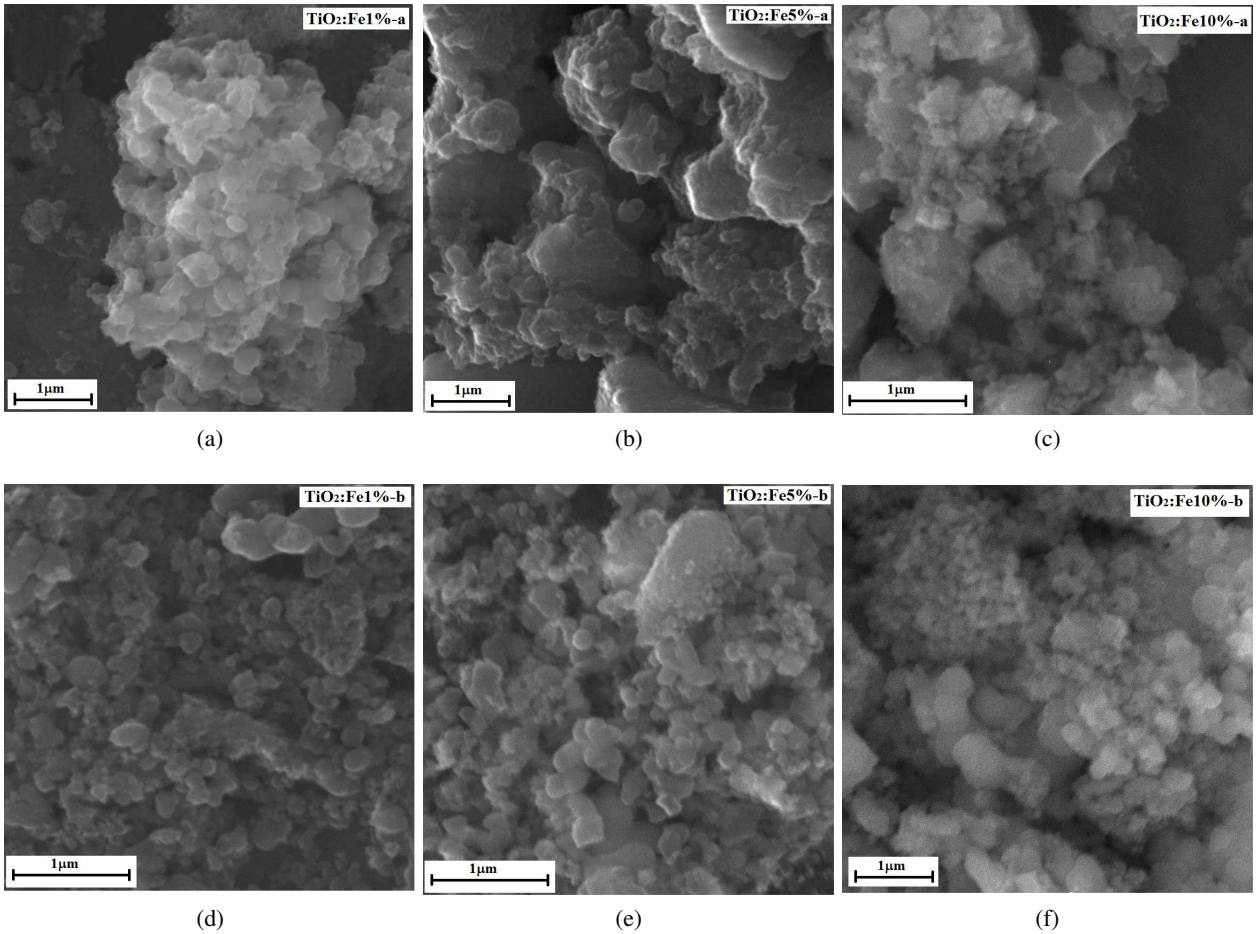

Figure 2. SEM micrographs of Fe doped titanium dioxide powders: a) TiO_2:Fe 1%-a, b) TiO_2: Fe 5%-a, c) TiO_2:Fe 10%-a, d) TiO_2:Fe 1%-b, e) TiO_2:Fe 5%-b and f) TiO_2:Fe 10%-b

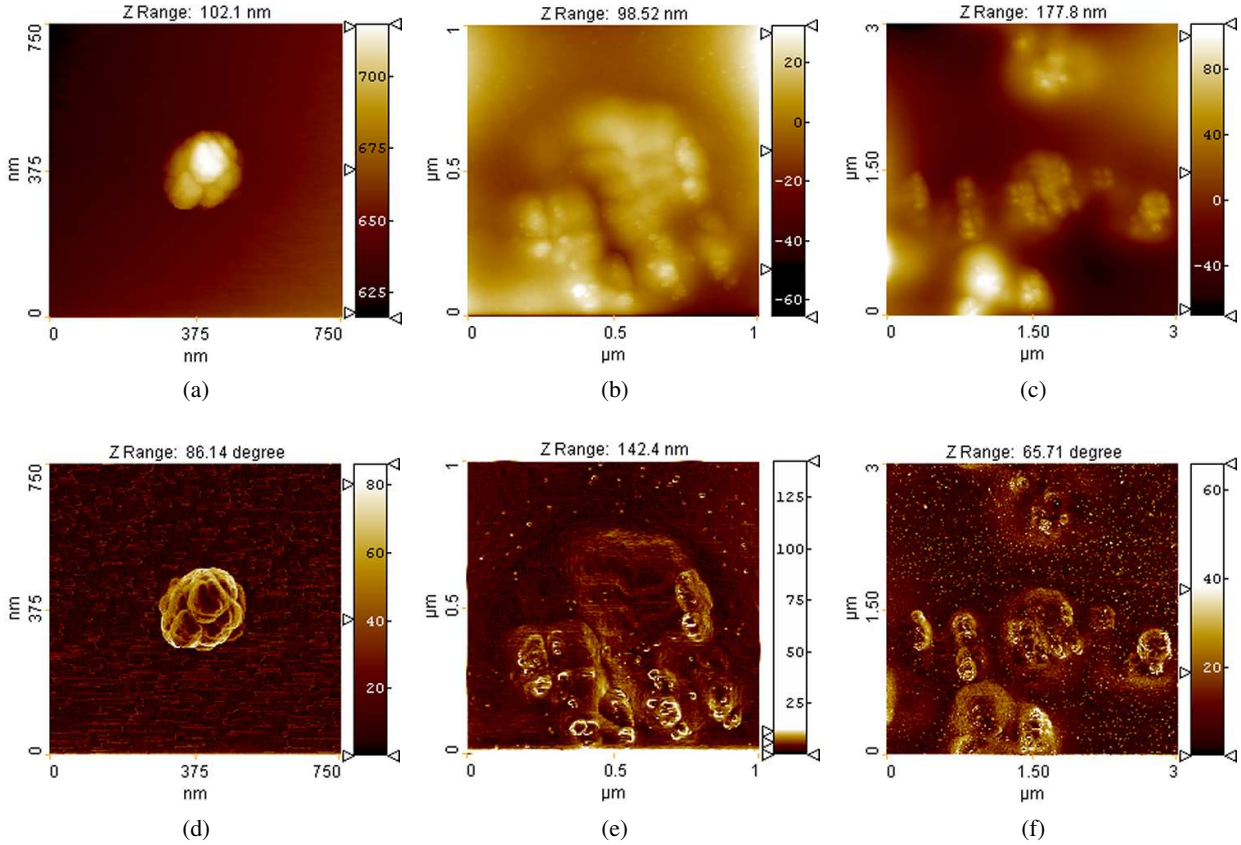

Figure 3. AFM micrographs - topography: a) TiO_2:Fe 1%-a, b) TiO_2: Fe 5%-a, c) TiO_2:Fe 10%-a and AFM micrographs - Sobel transform: d) TiO_2:Fe 1%-a, e) TiO_2:Fe 5%-a, f) TiO_2:Fe 10%-a

2.2. AFM, SEM and XRD measurements

Atomic force microscopy (AFM) measurements were performed with Innova system from Bruker (formerly Veeco) in air, at temperature 23 °C and humidity 35% RH. In order to perform the imaging of magnetic properties of the investigated powders, such as the presence of magnetic domains, magnetic force microscopy (MFM) was used [20]. The measurements were performed using MESP-LC probes from Bruker [21,22]. The liftmode height was set to 40 nm, in order to obtain selective detection of the long range magnetic forces.

In order to perform the AFM measurements of the prepared Fe doped TiO_2 powders, the microscope glass was used as the substrate. The surface of the glass was covered with cyanoacrylate glue and left for few seconds for preliminary cure. A small quantity of the powder was carefully placed on the surface of the substrate and left for few minutes to cure the glue. Afterwards, the weakly attached grains of the powder were removed using pressured air, in order to avoid them to stick to the scanning tip. Such an approach allowed obtaining of small agglomerates and single grains on the surface.

Scanning electron microscopy (SEM) studies were performed with a tungsten cathode Vega II SBH (TESCAN) to examine the morphology of the prepared Fe doped TiO_2 powders.

X-ray diffraction patterns were recorded using powder on a Pulveraceous diffractometer Dron–2. Co radiation filtrated by Fe was applied.

2.3. Magnetic measurements

The magnetic measurements were performed using the 12 T SQUID magnetic properties measurement system by quantum design. The dependences of the magnetization as a function of temperature and magnetization as a function of applied magnetic field were studied. Measurements of the temperature dependence of magnetization were carried out in the wide temperature range (1.8–300 K) at 0.5 T magnetic field. The measurements were performed in two manners: zero field cooled (ZFC) and cooled field (CF) for the sample TiO_2:Fe 1% and zero field cooled only for others samples. Cooled field measurement was carried only once due to the similar results with the zero-cooled field measurement.

III. Results and discussion

3.1. Structural characterization

X-ray diffraction and scanning electron microscopy (SEM) were used to analyse the prepared TiO_2 powders. The X-ray spectrum of the TiO_2 annealed at 500 °C shows the diffraction pattern characteristic to anatase crystalline phase (see Fig. 1). A major peak corresponding to 101 reflections of the anatase phase of TiO_2 was

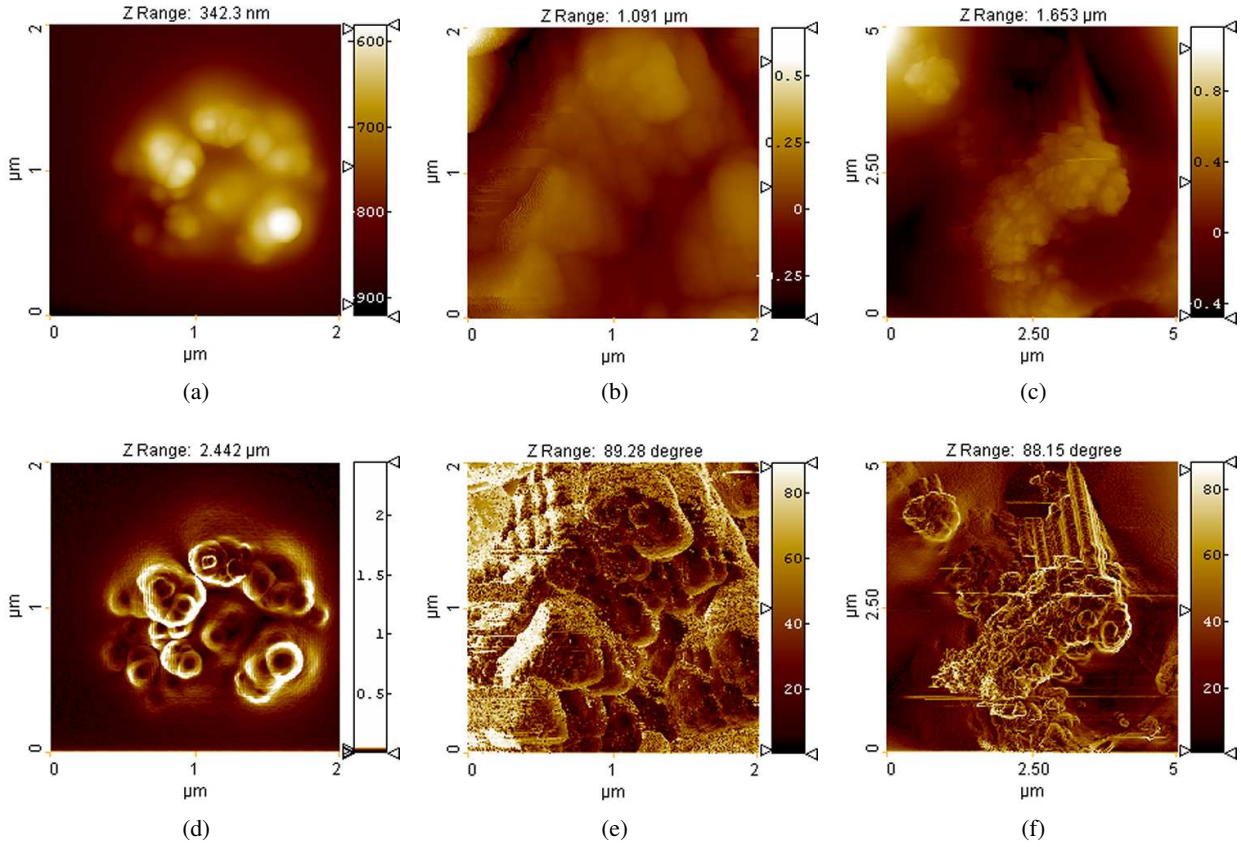

Figure 4. AFM micrographs - topography: a) TiO_2:Fe 1%-b, b) TiO_2: Fe 5%-b, c) TiO_2:Fe 10%-b and AFM micrographs - Sobel transform: d) TiO_2:Fe 1%-b, e) TiO_2:Fe 5%-b, f) TiO_2:Fe 10%-b

apparent at the angle of 29.45°. The X-ray results are in good agreement with other papers dedicated to TiO_2 [23].

The TiO_2:Fe powders were investigated by SEM technique. Morphologies of TiO_2:Fe revealed by SEM micrographs are shown in Fig. 2. The TiO_2:Fe samples appeared as agglomerates of smaller particles. The size of the obtained TiO_2:Fe particles is about 200–250 nm for TiO_2:Fe 1%-a and TiO_2:Fe 5%-b and about 350 nm for other powders, as it was confirmed by SEM.

Additionally the samples were measured with intermittent contact mode by AFM. The AFM images of TiO_2:Fe samples are presented in Figs. 3 and 4. The ranges of the diameter are as follows: 50–250 nm for TiO_2:Fe 1%-a, 25–150 nm for TiO_2:Fe 1%-b, 10–100 nm for TiO_2:Fe 5%-a, 20–180 nm for TiO_2:Fe 5%-b, 5–250 nm for TiO_2:Fe 10%-a and 5–200 nm for TiO_2:Fe 10%-b sample. The diameter distribution is not however Gaussian. Two fractions are apparent: the small one below 50 nm, and the large one above 100 nm. The amount of small grains appears to be relatively small, but it is difficult to estimate quantitatively, as such a small features may be hidden in the agglomerates and maintain undetected by SEM or AFM. Mapping the magnetic properties of single grains using MFM allowed estimating the size of magnetic domains (see Fig. 5). The obtained data enabled us to observe good correlation between grains and magnetic domains sizes. Additionally, no multiple- domains grains were observed. It should be noted, that along with Fe level increase, the grains created larger agglomerates. As the magnetic properties are weaker for materials containing more Fe component (see Magnetic study section), one can argue if such a behaviour may be related to domination of the adhesion forces over repulsive magnetic forces present between single magnetic domain grains. SPIP software was used for the data processing and analysis [21].

3.2. Magnetic study

The results of temperature dependence of mass magnetization for TiO_2:Fe powders are presented in Fig. 6. As seen, mass magnetization rises with Fe content. However, as it will be described below, mass susceptibility per Fe ion is decreasing with amount of iron (see Fig. 7).

The TiO_2:Fe 1%-a and TiO_2:Fe 1%-b samples demonstrate a peak at about 60 K which may relate with a superparamagnetic blocking temperature. Interpretation of this effect required the additional investigations of AC magnetization of these compounds. Other samples show the conventional paramagnetic dependence in the whole temperature range. One can suppose that the fraction of Fe and its oxides are too low and most of the Fe ions are located on the lattice interior. They are likely to undergo very week ferromagnetic exchange interaction (with paramagnetism or antiferromagnetism having

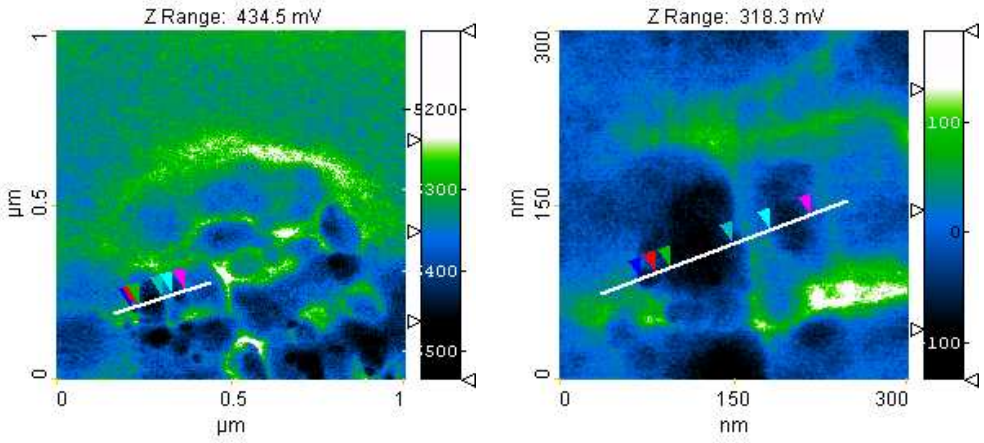

Figure 5. MFM of TiO_2 powder with Fe 5%-a, as an example

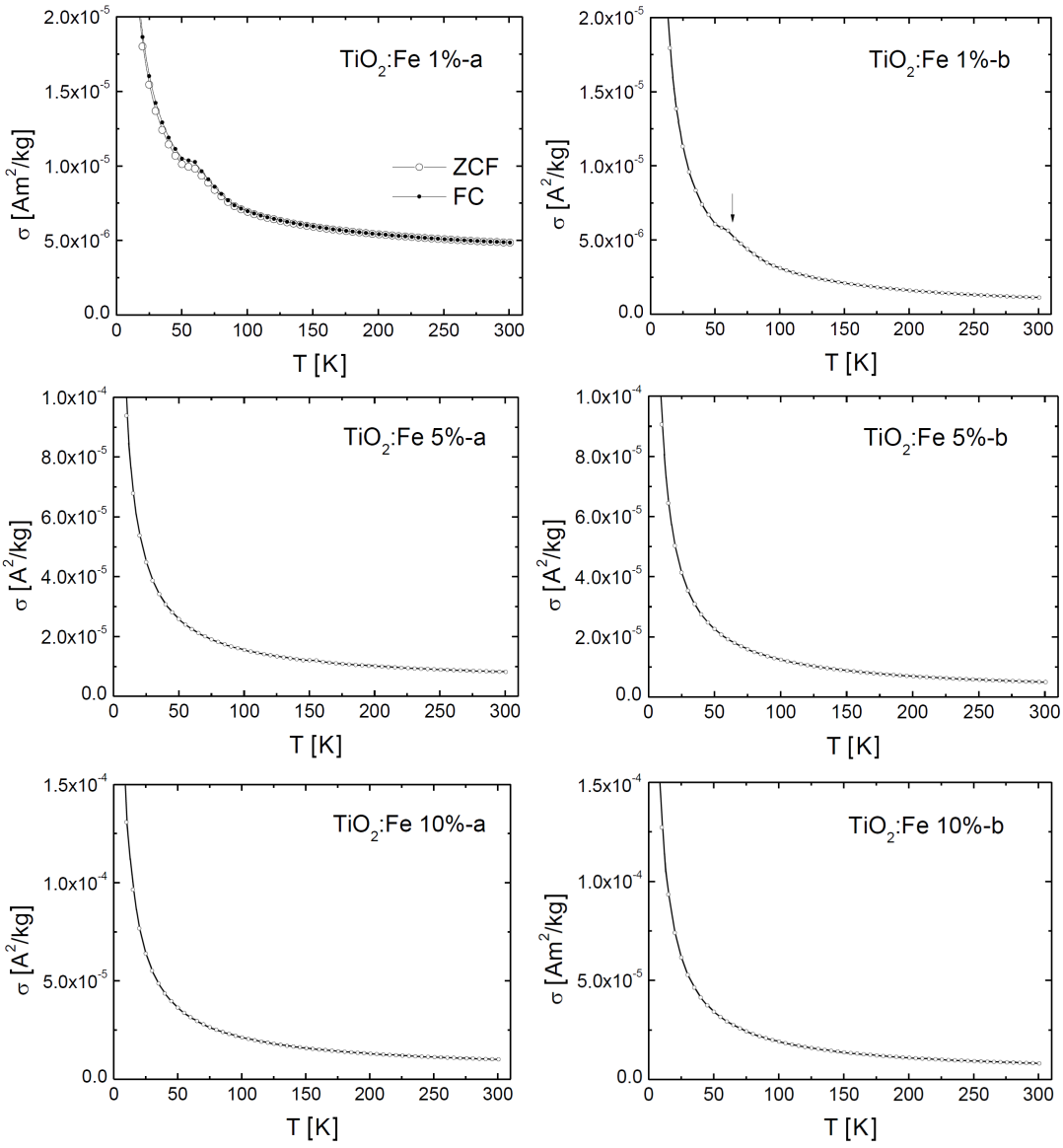

Figure 6. Temperature dependence of mass magnetization of TiO_2:Fe nanopowders measured at 0.5 T. For TiO_2:Fe 1%-a sample open circles correspond to the result obtained at zero field cooled; filled circles correspond to the data obtained at field cooled measurements

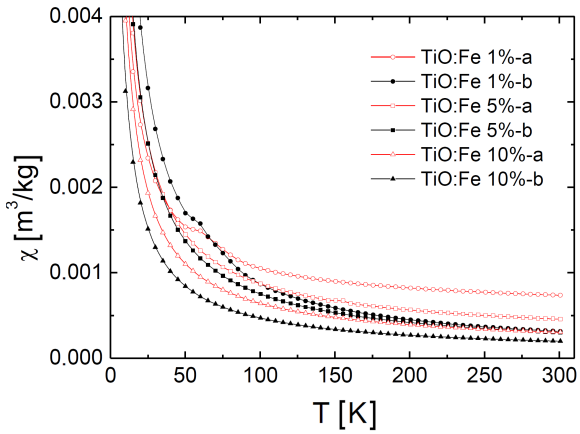

Figure 7. Temperature dependence of mass magnetic susceptibility per Fe ion of the TiO_2:Fe nanopowders with various level of Fe content at 0.5 T

dominance over ferromagnetism) and, thus, instead of ferromagnetic signal we have observed only paramagnetism in the samples [24].

Figure 8 represents the mass magnetization as a function of applied magnetic field measured at 300 K. The dependences revealed the superparamagnetic character for samples obtained by the first method with low Fe fraction. This character changed to the paramagnetic one with rising of iron content. The samples fabricated by the second method show the paramagnetic behaviour without any dependence on iron fraction. The observed dependencies may be ascribed in the following way. In the case of low iron content the small magnetic particles are well separated from each other revealing the dispersed single domain superparamagnetic behaviour. Such a structure manifests ferromagnetic-like dependence showed in Fig. 8 (TiO_2:Fe 1%-a). Rising of Fe content leads to formation of multi domain structure

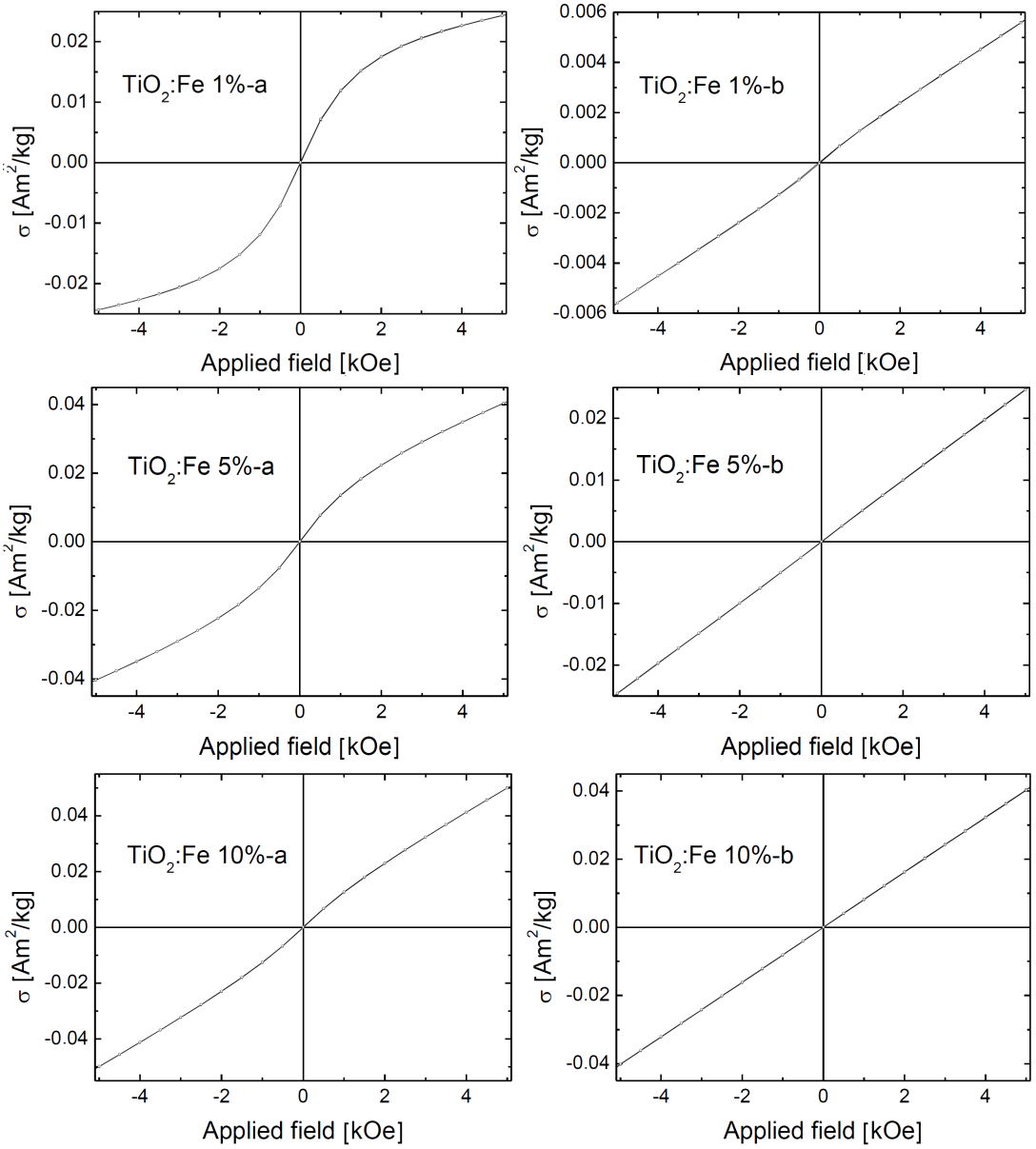

Figure 8. Mass magnetization as a function of magnetic field of TiO_2:Fe nanopowders at 300 K

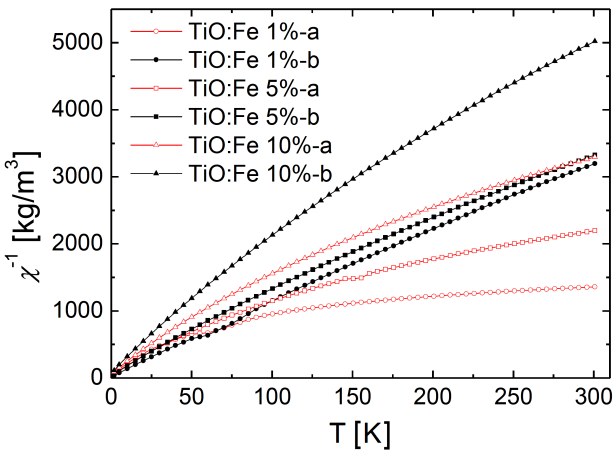

Figure 9. Temperature dependence of the reciprocal mass magnetic susceptibility per Fe ion of the TiO_2:Fe with various level of Fe content

of iron reach particles. In this case magnetization has a non-trivial dependence showing weak ferromagnetic-like and then paramagnetic-like character with rising of applied field.

All samples show the linear temperature dependence of the reciprocal susceptibility at high temperatures (see Fig. 9). It is easy to see that reciprocal susceptibility increases due to the iron doping. Such unexpected behaviour was observed in Fe and Ni doped TiO_2 films [25]. The authors in Ref. [25] relate this feature to the remark of Wokano *et al.* [26] assuming that rising of Ni content leads to decreasing of carrier density and its mobility.

The deviation from linearity appears when antiferromagnetic interaction dominates at lower temperatures. Such a character of dependences indicates the paramagnetic behaviour of susceptibility with relatively large values of the Curie temperature. In such systems, similarly as authors described in [23], paramagnetism appears because of the presence of isolated Fe^{3+} ions and the antiferromagnetic interaction might occur between Fe^{3+} dimmers or between Fe^{3+}–Fe^{3+} (or Fe^{3+}–O_2–Fe^{3+}) pair. Both of these contribute towards magnetization, while at high temperature the anti alignment of the spins in Fe^{3+} pair is broken and all spins align randomly showing characteristic of paramagnetism.

Due to the paramagnetic behaviour of all curves, the Curie-Weiss law can be applied to obtain the general magnetic parameters. Table 1 contains the Curie temperature, θ_p, and effective magnetic moment, μ_{eff}, of each sample obtained from the Curie-Weiss law for linear part of fitted curves (characteristics fitting on the dependences) presented in Fig. 9. Figure 9 shows the temperature dependence of the reciprocal magnetic susceptibility per Fe ion which was estimated using the values from Table 1.

The highest values of μ_{eff} correspond to the lowest Fe content. Moreover, these values for samples prepared by the first method are higher in comparison

Table 1. List of θ_p, and μ_{eff} for all samples obtained from curves showed in Fig. 9 (μ_{eff} taken at 300 K)

Sample	θ_p [K]	μ_{eff} [J/T]	μ_{eff} [μ_B]
TiO_2:Fe 1%-a	-582	$1.38 \cdot 10^{-24}$	0.149
TiO_2:Fe 5%-a	-206	$1.09 \cdot 10^{-24}$	0.117
TiO_2:Fe 10%-a	-117	$0.89 \cdot 10^{-24}$	0.096
TiO_2:Fe 1%-b	-21	$0.90 \cdot 10^{-24}$	0.097
TiO_2:Fe 5%-b	-47	$0.88 \cdot 10^{-24}$	0.095
TiO_2:Fe 10%-b	-75	$0.72 \cdot 10^{-24}$	0.078

with values of the nanopowders obtained by the second method. The relatively high negative values of θ_p suggest the antiferromagnetic ordering in all samples except for the TiO_2:Fe 1%-a and TiO_2:Fe 1%-b samples which have a peak at about 50 K that could be due to ferromagnetic ordering in these compounds. Independently from nanopowders preparation method, the values of effective magnetic moment per Fe ion are rather small in comparison to the value obtained within the Russell-Sounders coupling model, where μ_{eff} of Fe^{2+} is $4.54 \cdot 10^{-23}$ J/T (if $J = S$) or $6.21 \cdot 10^{-23}$ J/T (if $J = |L \pm S|$).

Figure 10 shows the θ_p and μ_{eff} as a function of Fe content for the samples obtained by both methods. Filled circles and squares correspond to the compounds obtained by the first method; hollow symbols correspond to the nanopowders synthesized by the second method.

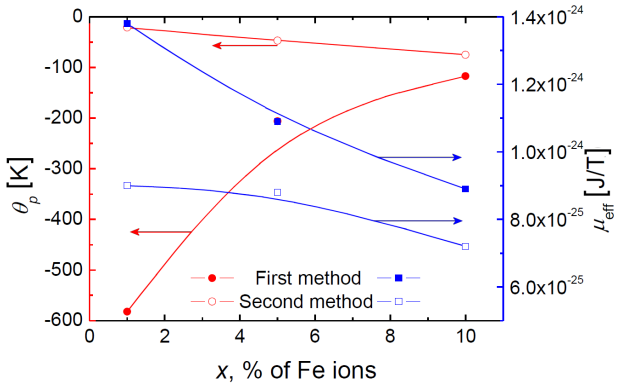

Figure 10. θ_p and μ_{eff} as a function of Fe content for the samples obtained by two methods. Red curves correspond to the θ_p values (left axes); blue curves correspond to the μ_{eff} (right axes)

As it can be seen, the samples obtained by the first method manifest strong dependences of Curie temperature and magnetic moment on the Fe content. At the same time, the compounds obtained by the second method show more moderate dependence. The θ_p of samples obtained by the first method rises with the Fe content but the samples obtained by the second method exhibit the decrease of θ_p on Fe concentration. However, the compounds obtained by both methods manifest the reduction of μ_{eff} with the concentration of Fe ions simultaneously. Actually, this effect was expected

to be opposite at least for μ_{eff} due to the magnetic nature of iron. Probably, this effect appears due to the reduction of mobility and number of charge carriers as a result of magnetic doping. An answer to this question requires an additional investigation of Hall-effect. Also, it should be taken into account that the TiO_2 has the diamagnetic nature thus some competition between ferromagnetic and diamagnetic particles is achieved. It is interesting that the highest discrepancy of values of θ_p and μ_{eff} was achieved at lowest Fe content for samples obtained by both methods. At the same time, this difference was rather reduced at higher concentrations of Fe.

IV. Conclusions

In summary, the magnetization as a function of temperature and applied magnetic field of TiO_2 nanopowders doped with 1, 5 and 10 mol% Fe and prepared by sol-gel method in two different ways has been measured in the wide temperature and magnetic field range. Except for the low Fe fraction samples, all compounds exhibit the paramagnetic behaviour with the negative Curie temperature that suggests the antiferromagnetic ordering. The samples with 1 and 5 mol% of Fe revealed superparamagnetic dependence on applied field with relatively low blocking temperature. Decreasing of mass susceptibility with the increasing of Fe content can be interpreted as a result of reduction of the mobility and number of charge carriers. The measurements showed that magnetic properties are more related to the nanopowders preparation method than to their grain size.

In order to better understand the influence of Fe ions on the magnetic properties of TiO_2, the additional studies of AC magnetization at low temperatures and Hall-effect are required.

Acknowledgement: The research was supported by Wroclaw Research Centre EIT+ under the project "The Application of Nanotechnology in Advanced Materials" – NanoMat (POIG.01.01.02-002/08) financed from the European Regional Development Fund (Operational Programme Innovative Economy, 1.1.2). The authors thank Dr. J. Warycha for SEM images of TiO_2.

References

1. J. Ananpattarachai, P. Kajitvichyanukul, S. Seraphin, "Visible light absorption ability and photocatalytic oxidation activity of various interstitial N-doped TiO_2 prepared from different nitrogen dopants", *J. Hazard. Mater.*, **168** (2009) 253–261.
2. A. Fujishima, K. Hashimoto, T. Watanabe, *TiO_2 Photocatalysis: Fundamentals and Applications*, BKC Inc., Tokyo, Japan, 1999.
3. Y. Zhang, Y. Chen, P. Westerhoff, J. Crittenden, "Impact of natural organic matter and divalent cations on the stability of aqueous nanoparticles", *Water Res.*, **43** (2009) 4249–4257.
4. I. Ganesh, A.K. Gupta, P.P. Kumar, P.S. Chandra Sekhar, K. Radha, G. Padmanabham, G. Sundararajan, "Preparation and characterization of Co-doped TiO_2 materials for solar light induced current and photocatalytic applications", *Mater. Chem. Phys.*, **135** (2012) 220–234.
5. H-W. Wang, H-C. Lin, C-H. Kuo, Y-L. Cheng, Y-C. Yeh, "Synthesis and photocatalysis of mesoporous anatase TiO_2 powders incorporated Ag nanoparticles", *J. Phys. Chem. Solids*, **69** (2008) 633–636.
6. Y. Lai, Y. Chen, H. Zhuang, C. Lin, "A facile method for synthesis of Ag/TiO_2 nanostructures", *Mater. Lett.*, **62** (2008) 3688–3690.
7. S.A. Amin, M. Pazouk, A. Hosseinnia, "Synthesis of TiO_2-Ag nanocomposite with sol-gel method and investigation of its antibacterial activity against E. coli", *Powder Technol.*, **196** (2009) 241–245.
8. X. S. Li, G. E. Fryxell, C. Wang, M. H. Engelhard, "The synthesis of Ag-doped mesoporous TiO_2", *Micropor. Mesopor. Mater.*, **111** (2008) 639–642.
9. Q-H. Wu, A. Fortunelli, G. Granozzi, "Preparation, characterisation and structure of Ti and Al ultrathin oxide films on metals", *Int. Rev. Phys. Chem.*, **28** (2009) 517–576.
10. M. Cernea, C. Valsangiacom, R. Trusca, F. Vasiliu, "Synthesis of iron-doped anatase -TiO_2 powders by a particulate sol-gel route", *J. Optoelectron. Adv. Mater.*, **9** (2007) 2648–2652.
11. K. Ranjit, B. Viswanathan, "Synthesis, characterization and photocatalytic properties of iron-doped TiO_2 catalysts", *J. Photochem. Photobiol. A: Chem.*, **108** (1997) 79–84.
12. M. Litter, J. Navio, "Photocatalytic properties of iron-doped titania semiconductors", *J. Photochem. Photobiol. A: Chem.*, **98** (1996) 171–181.
13. N.J. Peill, M.R. Hoffmann, "Mathematical model of a photocatalytic fiber- optic cable reactor for heterogeneous photocatalysis", *Environ. Sci. Technol.*, **32** (1998) 398–404.
14. N. Nasralla, M. Yeganeh, Y. Astuti, S. Piticharoenphuna, N. Shahtahmasebi, A. Kompany, M. Karimipour, B.G. Mendis, N.R.J. Poolton, L. Šiller, "Structural and spectroscopic study of Fe-doped TiO_2 nanoparticles prepared by sol-gel method", *Sci. Iranica F*, **20** (2013) 1018.
15. I. Ganesh, P.P. Kumar, A. K. Gupta, P.S.C. Sekhar, K. Radha, G. Padmanabham, G. Sundararajan, "Preparation and characterization of Fe-doped TiO_2 powders for solar light response and photocatalytic applications", *Process. Appl. Ceram.*, **6** (2012) 21–36.
16. K.S. Yao, D.Y. Wang, J.J. Yan, L.Y. Yang, W.S. Chen, "Photocatalytic bactericidal effect of TiO_2 thin film on plant pathogens", *Surf. Coat. Technol.*, **201** (2007) 6882–6885.
17. T.C. Cheng, K.S. Yao, N. Yeh, C.I. Chang, H.C. Hsu, Y.T. Chien, C.Y. Chang, "Visible light activated bactericidal effect of TiO_2/Fe_3O_4 magnetic particles

on fish pathogens", *Surf. Coat. Technol.*, **204** (2009) 1141–1144.
18. Y. Lui, J.H. Wei, R. Xiong, C.X. Pan, J. Shi, "Enhanced visible light photocatalytic properties of Fe-doped TiO_2 nanorod clusters and monodispersed nanoparticles", *Appl. Surf. Sci.*, **257** (2011) 8121–8126.
19. Z. Shi, X. Zhang, S. Yao, "Preparation and photocatalytic activity of TiO_2 nanoparticles co-doped with Fe and La", *Particuology*, **9** (2011) 260–264.
20. S.F. Alvarado, "Understanding magnetic force microscopy", *Exp. Techniques*, 383 (1990) 373–383.
21. *Probes and Accessories*, Bruker Corporation, (2011) 96-97.
22. S.S. Kamble, A. Sikora, S.T. Pawar, N.N. Maldar, L.P. Deshmukh, "Cobalt sulfide thin films: chemical growth, reaction kinetics and microstructural analysis", *J. Alloys Compd.*, **623** (2015) 466–472.
23. M. Vijay, V. Selvarajan, K.P. Sreekumar, Y. Jiaguo, L. Shengwei, "Characterization and visible light photocatalytic properties of nanocrystalline TiO_2 synthesized by reactive plasma processing", *Solar Energy Mater. Solar Cells*, **93** (2009) 1540–1549.
24. B. Choudhury, R. Verma, A. Chodhury, "Oxygen defect assisted paramagnetic to ferromagnetic conversion in Fe doped TiO_2 nanoparticles", *RSC Advances*, **4** (2014) 29314.
25. N.H. Hong, J. Sakai, W. Prellier, "Distribution of dopant in Fe:TiO_2 and Ni:TiO_2 thin films", *J. Magn. Magn. Mater.*, **281** (2004) 347–352.
26. T. Wakano, N. Fujimura, Y. Morinaga, N. Abe, A. Ashida, T. Ito, "Magnetic and magneto-transport properties of ZnO:Ni films", *Physica E*, **10** (2001) 260–264.